JOURNAL OF AGRICULTURAL AND FOOD CHEMISTRY

Novel Fluorometric Assay for Hydroxyl Radical Scavenging Capacity (HOSC) Estimation

JEFFREY MOORE,† JUN-JIE YIN,§ AND LIANGLI (LUCY) YU*,†

Department of Nutrition and Food Science, University of Maryland, College Park, Maryland 20742, and Center for Food Safety and Applied Nutrition, U.S. Food and Drug Administration, College Park, Maryland 20740

A novel fluorometric method was developed and validated for hydroxyl radical scavenging capacity (HOSC) estimation using fluorescein as the probe. A constant flux of pure hydroxyl radical is generated under physiological pH using a Fenton-like Fe^{3+}/H_2O_2 reaction. The generation of pure hydroxyl radicals under the experimental conditions was evaluated and confirmed using electron spin resonance with DMPO spin-trapping measurements. The hydroxyl radical scavenging capacity of a selected antioxidant sample is quantified by measuring the area under the fluorescence decay curve with or without the presence of the antioxidant and expressed as Trolox equivalents per unit of the antioxidant. The assay may be performed using a plate reader with a fluorescence detector for high-throughput measurements. The assay was validated for linearity, precision, accuracy, reproducibility, and its correlation with a popular peroxyl radical scavenging capacity assay using selected pure antioxidant compounds and botanical extracts. This method may provide researchers in the food, nutrition, and medical fields an easy to use protocol to evaluate free radical scavenging capacity of pure antioxidants and natural extracts in vitro against the very reactive hydroxyl radical, which may be linked to numerous degenerative diseases and conditions.

KEYWORDS: Hydroxyl radical; antioxidant; ferric iron; Fenton-like reaction; fluorescein; electron spin resonance

INTRODUCTION

Reactive oxygen species (ROS) and their roles in human pathology have recently been of great interest in the area of health promotion and disease prevention. ROS contribute to oxidative stress, which is linked to numerous degenerative conditions including carcinogenesis (*1*), cardiovascular disease (*2*), inflammation (*3*), Alzheimer's disease (*4*), Parkinson's disease (*5*), diabetes (*6*), and aging (*7*). Mechanisms involved in the role of ROS and oxidative stress in disease development may include alteration of important biomolecules, causing oxidative modification of proteins (*8*), oxidation of lipids (*9*), stand breaks and modification to nucleic acids (*10*), modulation of gene expression through activation of redox-sensitive transcription factors (*11*, *12*), and modulation of inflammatory responses through signal transduction (*3*). Growing evidence suggests that dietary antioxidants may protect important biological molecules from oxidative damage and reduce the risk of numerous chronic diseases related to advancing age (*13*). This has created a demand of simple, reliable, high-thoughput in vitro method(s) measured under physiologically relevant conditions for the rapid screening and development of potential dietary antioxidants, as suggested by a recent "white paper" review from the First International Congress on Antioxidant Methods sponsored by the American Chemical Society (*14*).

Of the physiologically relevant ROS, the hydroxyl radical (•OH) is extremely reactive with almost every type of biomolecules and is possibly the most reactive chemical species known (*15*). The presence and pathological role of •OH in vivo have been demonstrated and include direct attack of proteins and nucleic acids (*10*, *16*). Hydroxyl radicals may serve as an excellent target to investigate dietary antioxidants for their potential to directly react with and quench free radicals and protect important biomolecules from radical-mediated damage.

One of the most important properties of an ideal •OH scavenging capacity assay is a source of •OH without interference from other ROS. There are five categories of •OH-generating systems described by previous researchers based on the reaction used for radical generation including (1) the classic Fenton reaction including the pH 7.4 buffered ferric iron−EDTA/ascorbic acid/H_2O_2 system used in the "deoxyribose assay" (*17*) and several alternatives (*18*−*20*); (2) the superoxide-driven Fenton reaction known also as the Haber−Wilstatter or the Haber−Weiss reaction (*21*−*24*) using the hypoxanthine/xanthine oxidase system to generate •OH and its alternative proposed by Yang and Guo (*25*); (3) use of "Fenton-like" reagents to produce •OH including the Co(II)/H_2O_2 (*26*) and the Cu(II)/H_2O_2 systems (*27*, *28*); (4) pulse radiolysis of water to generate •OH (*15*); and (5) "photo-Fenton" systems using photosensitizers to create

* Corresponding author [telephone (301) 405-0761; fax (301) 314-3313; e-mail lyu5@umd.edu].
† University of Maryland.
§ U.S. Food and Drug Administration.

10.1021/jf052555p CCC: $33.50
Published on Web 01/12/2006

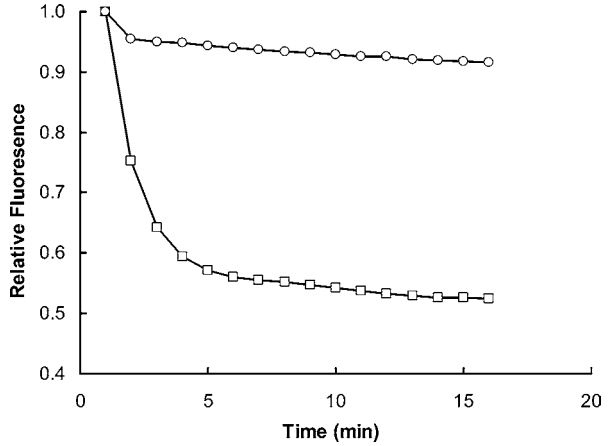

Figure 1. Fluorescein (FL) degradation by •OH generated from Fe(III)/H_2O_2/ascorbic acid in different buffering systems. Reactions were carried out in 96-well plates, and fluorescence was measured every minute using a plate reader with a fluorescence detector with the following initial reaction concentrations: (○) 5.26×10^{-8} M FL, 42.5 mM sodium phosphate buffer (pH 7.4), 25 μM Fe(III), 26.5 mM H_2O_2, 100 μM ascorbic acid, 100 μM EDTA, 5% (v/v) acetone, final reaction pH remained 7.4; (□) 5.26×10^{-8} M FL, 30 mM potassium phosphate buffer (pH 7.4), 25 μM Fe(III), 26.5 mM H_2O_2, 100 μM ascorbic acid, 100 μM EDTA, 5% (v/v) acetone, final reaction pH was changed to 6.0.

•OH (*29*). The radiolysis and photosensitization systems do not measure the •OH scavenging capacity under physiologically relevant conditions. The hypoxanthine/xanthine oxidase system generates superoxide ($O_2^{\bullet -}$) in addition to •OH and may have interference from enzyme inhibitors, which result in overestimation of •OH scavenging capacity.

The deoxyribose method is one of the most commonly used methods for •OH scavenging capacity estimation in the aqueous phase (*30*−*33*). This method uses the classic Fenton reaction to generate •OH and degrade 2-deoxyribose to "malondialdehyde-like" products, which form a chromagen with thiobarbituric acid detectable at 532 nm. However, our preliminary study observed two issues with this method. First, a drop in pH from 7.4 to 6.0 was found during the initial reaction, and attempting to increase the system buffering capacity to maintain pH 7.4 resulted in no detectable chromagen. Additional experiments using fluorescein (FL) as the probe instead of deoxyribose explained these observations, showing that FL was rapidly degraded at pH 6.0, whereas almost no FL was degraded while at pH 7.4 (**Figure 1**), suggesting that the deoxyribose method may not generate •OH at physiological pH. This finding was supported by observations of other researchers (*25*, *26*, *34*−*36*). The second issue with this assay was an extraction solvent interference. When the assay was run with 50% acetone solution of antioxidants, no significant difference was found between sample and blank measurements. UV spectrum analyses showed that the chromagen absorption spectrum was altered, with the peak at 532 nm significantly decreased (**Figure 2**) in the presence of acetone. This could possibly be due to the competition of the carbonyl group in acetone molecules with the malondialdehyde-like compounds for the reaction with thiobarbituric acid, thereby forming a different chromagen molecule with altered absorption spectra.

This study was undertaken to determine the optimal procedure for •OH scavenging capacity assay under physiological pH. This method may meet the needs of antioxidant researchers in the food, nutrition, health, and medical fields.

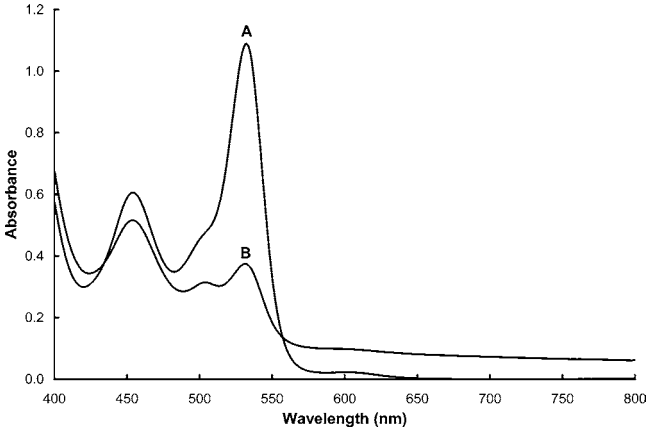

Figure 2. Absorption spectra of deoxyribose assay chromagen (**A**) without and (**B**) with acetone. Reaction conditions included the following initial reaction concentrations and conditions: 2.8 mM 2-deoxyribose, 200 μM $FeCl_3$, and 100 μM EDTA premixed, 10 mM potassium phosphate buffer at pH 7.4, 2.8 mM H_2O_2 prepared fresh, 5% (v/v) acetone or water as blanks, and 100 μM ascorbic acid made fresh. These reaction mixtures were heated for 60 min at 37 °C in a water bath followed by the addition of 1 mL of 2.8% trichloroacetic acid and 1 mL of 1% thiobarbituric acid and heating in a water bath at 80 °C for 20 min. Reaction vessels were then cooled in an ice–water bath for 15 min and centrifuged for 10 min, and absorbance spectra were recorded from 800 to 400 nm.

MATERIALS AND METHODS

Chemicals and Reagents. Fluorescein (FL), iron(III) chloride, iron(II) sulfate heptahydrate, copper(II) sulfate, cobalt(II) fluoride tetrahydrate, picolinic acid, disodium ethylenediaminetetraacetate (EDTA), 6-hydroxy-2,5,7,8-tetramethylchroman-2-carboxylic acid (Trolox), 5,5-dimethyl *N*-oxide pyrroline (DMPO), thiobarbituric acid, trichloroacetic acid, and ascorbic acid (vitamin C) were purchased from Sigma-Aldrich. Thirty percent H_2O_2 was purchased from Fischer Scientific. β-Cyclodextrin (RMCD) was purchased from Cyclolab R&D Ltd. (Budapest, Hungary). Ultrapure water was used for all experiments from an ELGA (Lowell, MA) A Purelab Ultra Genetic polishing system was used with <5 ppb of TOC and resistivity of 18.2 mΩ. All other chemicals and solvents were of the highest commercial grade and used without further purification.

Reagent Preparation. A 1×10^{-5} M stock fluorescein (FL) solution was prepared in sodium phosphate buffer (75 mM, pH 7.4) and stored at 0 °C for future use. Stock FL solution was diluted to 9.28×10^{-8} M with 75 mM sodium phosphate buffer (pH 7.4) fresh for each assay run. Iron(III) chloride, iron(II) sulfate, and copper(II) sulfate solutions were prepared daily in ultrapure water. A cobalt solution was prepared daily by dissolving 15.7 mg of Co(II) fluoride tetrahydrate and 20 mg of picolinic acid in 10 mL of ultrapure water. A 0.1990 M H_2O_2 solution was prepared fresh for each assay by diluting 30% H_2O_2 with ultrapure water. A 7% (v/w) RMCD solution prepared was in ultrapure water.

Natural Extracts Preparation. Extracts of natural materials with known antioxidant properties including cinnamon, hard wheat bran, and soft wheat grain were included in our electron spin resonance (ESR) experiments and our new hydroxyl radical scavenging capacity (HOSC) assay to demonstrate their •OH scavenging capacities. Samples were ground to 20 mesh using a micromill (Scienceware, Pequannock, NJ) and were extracted with 50% acetone for 24 h in the dark, under nitrogen, at ambient temperature and pressure. All extracts were stored in the dark under nitrogen at room temperature.

Standards Preparation. Standard solutions of compounds with known radical scavenging activity including Trolox and *p*-coumaric, caffeic, ferulic, syringic, and 4-hydroxybenzoic acids were prepared in 50% acetone and stored in the dark under nitrogen. Trolox standards were prepared at the following concentrations: 20, 40, 60, 80, and 100 μM in 50% acetone for HOSC assay; 14, 44, 88, 116, and 160 μM in 50% acetone for the deoxyribose assay; and other concentrations in 50% acetone as indicated in figure captions.

HOSC Fluorometric •OH Scavenging Capacity Assay. Assay reactions were carried out in FluroNunc black 96-well polystyrene plates from Fischer Scientific and analyzed using a Victor^3 multilabel plate reader (Perkin-Elmer, Turku, Finland) with an excitation wavelength of 485 nm, emission wavelength of 535 nm, and 0.1 s read time for each well with each plate read once per minute for 3 h. The reaction mixtures contained 170 μL of 9.28×10^{-8} M FL prepared in 75 mM sodium phosphate buffer (pH 7.4), 30 μL of blank or extract or standard, 40 μL of 0.1990 M H_2O_2, and 60 μL of 3.43 mM $FeCl_3$, added in that order. Trolox concentrations of 20, 40, 60, 80, and 100 μM were used as standards. HOSC values were calculated using the regression equation between Trolox concentration and net area under the FL decay curve as described by Ou and others (*37*). Area under the curve (AUC) values were calculated as

$$\mathrm{AUC} = 0.5 + f_1/f_0 + f_2/f_0 + f_3/f_0 + ... + f_{i-1}/f_0 + 0.5(f_i/f_0)$$

where f_0 is the initial fluorescence reading at 0 min and f_i is the final fluorescence reading. The net AUC is calculated by subtracting the AUC of the blank from the AUC of the sample. Relative HOSC values were expressed as micromoles of Trolox equivalents (TE) per gram of material and micromoles of TE per micromole of compound for pure compounds, with both calculations shown below.

$$\text{relative HOSC value for pure compounds} = [(\mathrm{AUC}_{\mathrm{sample}} - \mathrm{AUC}_{\mathrm{blank}})/(\mathrm{AUC}_{\mathrm{Trolox}} - \mathrm{AUC}_{\mathrm{blank}})] \times (\text{molarity of Trolox/molariy of sample})$$

$$\text{relative HOSC value for natural extracts} = [(\mathrm{AUC}_{\mathrm{sample}} - \mathrm{AUC}_{\mathrm{blank}})/(\mathrm{AUC}_{\mathrm{Trolox}} - \mathrm{AUC}_{\mathrm{blank}})] \times (\text{molarity of Trolox/mass of sample})$$

Deoxyribose Assay. The deoxyribose assay was conducted according to a previously described protocol (*17*). Initial reaction concentrations were 2.8 mM 2-deoxyribose, 200 μM $FeCl_3$, and 100 μM EDTA premixed, 10 mM potassium phosphate buffer at pH 7.4, 2.8 mM H_2O_2 prepared fresh, 5% (v/v) acetone as blank, and 100 μM ascorbic acid made fresh. The total volume was 1.2 mL for all reaction mixtures. The reaction mixtures were kept for 60 min at 37 °C followed by the addition of 1 mL of 2.8% trichloroacetic acid and 1 mL of 1% thiobarbituric acid and heating in a water bath at 80 °C for 20 min. Reaction vessels were then cooled in ice−water for 15 min and centrifuged for 10 min, and absorbance was read at 532 nm with a Genesys 20 spectrophotometer (Thermo Spectronic, Rochester, NY). Absorption spectra were taken with a UV-1601 spectrophotometer (Shimadzu, Columbia, MD).

Fluorescein Degradation Using a Deoxyribose •OH-Generating System under Two pH Values. Experimental conditions included a •OH-generating system reaction used in deoxyribose assay (*17*) with fluorescein probe. The final reaction pH 7.4 experiment included the following initial reaction concentrations: 5.26×10^{-8} M FL, 42.5 mM sodium phosphate buffer (pH 7.4), 25 μM $FeCl_3$, 26.5 mM H_2O_2, 100 μM ascorbic acid, 100 μM EDTA, and 5% (v/v) acetone. The final reaction pH 6.0 experiment was carried out under the same conditions except the buffering system, which was 30 mM (initial reaction concentration) potassium phosphate buffer (pH 7.4). Fluorescence measurements were made using the same equipment and conditions as used in the HOSC assay.

Oxygen Radical Absorbance Capacity (ORAC) Assay. The ORAC assay was conducted using FL as the fluorescent probe and a Victor^3 multilabel plate reader (Perkin-Elmer) according to a laboratory protocol (*37*). Standards were prepared in 50% acetone, whereas all other reagents were prepared in 75 mM sodium phosphate buffer (pH 7.4). The initial reaction mixture contained 225 μL of 8.16×10^{-8} M FL, 30 μL of standard or 50% acetone for blanks, and 25 μL of 0.6 M AAPH for blank. The fluorescence of the assay mixture was recorded every minute for 2 h at ambient temperature. Excitation and emission wavelengths were 485 and 535 nm, respectively. TE were calculated for samples based on the same AUC calculations used for the ORAC assay (*38*) with results expressed as micromoles of TE per gram of material for natural extracts and as micromoles of TE per micromole of compound for pure standards.

ESR Spin-Trapping Assay. ROS generation and •OH scavenging were examined by an ESR method using DMPO as the trapping agent. The reaction mixtures contained 75 μL of 85 mM sodium phosphate buffer (pH 7.4), 10 μL of 1.5 M DMPO, 15 μL of blank or extract or standard, 20 μL of 0.1990 M H_2O_2, and 30 μL of 3.43 mM $FeCl_3$, added in that order. Initial reaction concentrations were 42.5 mM sodium phosphate buffer, 26.53 mM H_2O_2, 0.686 mM $FeCl_3$, and 10% (v/v) sample extract or solvent blank. All reaction mixtures were vortexed and held for 2 min before analysis using a Varian E-109X-Band ESR spectrometer (Varian, Inc., Palo Alto, CA). Conventional ESR spectra were recorded with 15 mW incident microwave power and 100 kHz field modulation of 1 G at ambient temperature. Under the testing conditions, •OH signal strength was proportional to its concentration.

Statistical Analysis. Data were reported as mean ± SD for triplicate determinations. ANOVA and Tukey's tests were performed (SPSS for Windows, version rel. 10.0.5, 1999, SPSS Inc., Chicago, IL) to identify differences among means. A two-tailed Pearson's correlation test was conducted to determine the correlations among means. Statistical significance was declared at $P \leq 0.05$.

RESULTS AND DISCUSSION

It is widely accepted that an ideal radical scavenging activity assay should have the following characteristics: (1) simplicity; (2) production of a steady flux of pure radicals throughout the assay time frame from a biologically relevant radical-generating system; (3) utilization of a physiological reaction pH; (4) utilization of equipment commonly available in antioxidant research laboratories; (5) a definite endpoint and chemical mechanism; (6) compatibility with commonly used extraction solvents; (7) validity for performance characteristics; and (8) adaptability to "high-throughput" analysis (*14*). In the present study, a novel fluorometric procedure was developed and validated for •OH scavenging capacity estimation.

•OH-Generating System Selection. Four •OH-generating systems were evaluated for their capacities to generate a steady flux of pure •OH under physiological pH, using FL as the ROS-detecting probe. These systems included the superoxide-driven Fenton reaction (*25*) and "Fenton-like" reagents including Co(II)/H_2O_2 (*26*), Cu(II)/H_2O_2 (*27*, *28*), and Fe(III)/H_2O_2, a system that has been shown to cause DNA stand breakage (*39*) and presumably produce •OH (*40*) at physiological pH. The Co(II)/H_2O_2, Cu(II)/H_2O_2, and Fe(III)/H_2O_2 systems caused a significant drop in FL fluorescence, indicating the presence of ROS and their attack on FL, whereas the superoxide-driven Fenton system under the experimental conditions caused no degradation to FL at pH 7.4, suggesting little ROS formation (**Figure 3**). These results suggested that Co(II)/H_2O_2, Cu(II)/H_2O_2, and Fe(III)/H_2O_2 systems may be suitable choices for •OH scavenging capacity assays.

It is widely accepted that Co(II), Cu(II), and Fe(III), in combination with H_2O_2, called Fenton-like reagents, generate ROS, but the exact species formed and their mechanisms have been greatly debated in the literature (*41*, *42*). Further investigations were conducted with the Co(II)/H_2O_2, Cu(II)/H_2O_2, and Fe(III)/H_2O_2 systems to verify the ROS generated under the experimental conditions with ESR using DMPO as the spin-trapping agent. The time-dependent ESR spectra of DMPO spin adducts formed during the Co(II)/H_2O_2 reaction (**Figure 4a**) showed a mixture of DMPO/•OH and possibly DMPO/$O_2^{\bullet-}$ adducts formed at pH 7.4 (*43*). These results were supported by the conclusions of Kadiiska and others (*44*), who found a mixture of •OH and $O_2^{\bullet-}$ generated by this system at physiological pH, and others who have proposed that ROS besides •OH could be generated by this system at physiological pH (*45*−

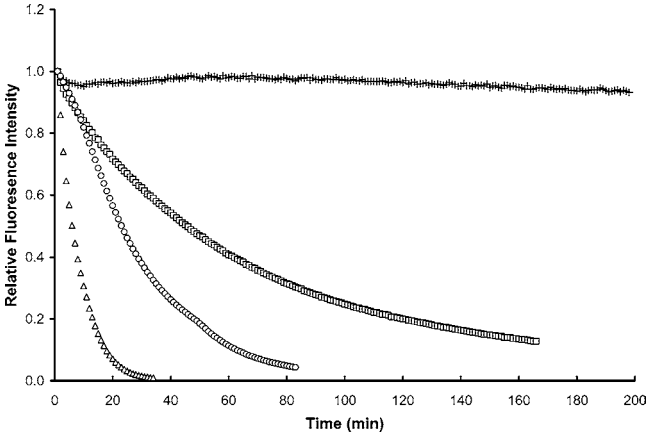

Figure 3. Fluorescent decay curves of fluorescein with selected Fenton-like reaction systems. Fluorescence decay curves of fluorescein were prepared to compare and evaluate different proposed Fenton-like hydroxyl radical generating systems. All reactions were performed in 96-well plates with the initial reaction concentrations of 42.5 mM phosphate buffer (pH 7.4), 5.26×10^{-8} M FL, and 5% (v/v) acetone, added in that order, followed by (□) 0.343 mM Fe(III), 26.5 mM H_2O_2; (△) 0.95 mM Cu(II), 26.5 mM H_2O_2; (+) 0.08 mM Fe(II), 0.08 mM EDTA; and (○) 230 μM Co(II), 2.75×10^{-2} M H_2O_2.

47). Similarly for the Cu(II)/H_2O_2 reaction, a mixture of DMPO/•OH and possibly DMPO/$O_2^{\bullet-}$ adducts was observed in the time-dependent ESR spectra of DMPO adducts formed at pH 7.4 (**Figure 4b**). This observation was supported by the previous finding of ROS besides •OH generated by the Cu(II)/H_2O_2 system at physiological pH (*48*−*50*). The results for both the Co(II)/H_2O_2 and Cu(II)/H_2O_2 systems indicated that they would not produce a steady flux of pure •OH and, therefore, were not suitable for a •OH scavenging capacity estimation assay.

The time-dependent ESR spectra of DMPO spin adducts formed during the Fe(III)/H_2O_2 reaction at pH 7.4 are shown in **Figure 4c**. This figure shows a typical DMPO/•OH adduct signal with a characteristic quartet signal intensity ratio of 1:2:2:1 and hyperfine coupling $a_N = a_H = 14.7$ G (*51*), which is consistently present throughout the entire 30 min testing time frame. This indicated that the tested Fe(III)/H_2O_2 system with no chelating agent was capable of producing a steady flux of pure •OH, making it an ideal •OH-generating system for a •OH scavenging capacity assay. Whereas ferrous and not ferric iron is the oxidation state of iron typically associated with the classic Fenton reaction, numerous researchers have reported the generation of ROS from the ferric reaction including Tachon (*39*), who reported DNA degradation in a buffered system, and Kocha and others (*40*), who reported aromatic hydroxylation of benzoate using EDTA chelated ferric iron and H_2O_2 in a pH 7.2 buffered system. In addition, other researchers (*52*−*54*) have reported the generation of •OH from chelated ferric iron/H_2O_2, using ESR with DMPO as a spin-trapping agent. The mechanism of this reaction and even the classic Fenton reaction has been debated over the years and is still not completely understood (*55*). The complexity in analyzing these mechanisms is attributed to the competition of mechanisms depending on reaction conditions such as pH, solvents, ligands, the presence of oxidizable organic substrates, and the extremely short lives of many of the reactive species (*56*).

A commonly accepted mechanism for this reaction involves a radical chain reaction with Fe(II), HO•, $O_2^{\bullet-}$, and •OOH as propagating species and was originally proposed by Barb and others (*57*) and is often referred to as the superoxide- or Haber−Weiss-driven Fenton reaction. This reaction was originally thought to involve the direct oxidation of Fe(III) by H_2O_2 to form $O_2^{\bullet-}$ under basic conditions or •OOH under acidic conditions, but was later hypothesized to involve an intermediate ferric−hydroperoxy complex (*53*). This mechanism under acidic conditions outlined by Perez-Benito (*58*) begins with the reaction of Fe(III) and H_2O_2 to form an intermediate, the ferric−hydroperoxy complex, $[Fe(III)-OOH]^{2+}$, which decomposes to Fe^{2+} and •OOH, with ferrous iron reacting with H_2O_2 to yield •OH. This mechanism has been supported by De Laat and Gallard's kinetic study (*59*). Ensing and others (*56*), however, using DFT calculations and Car-Parrinello molecular dynamic simulations have shown that the probable fate of the $[Fe(III)-OOH]^{2+}$ intermediate is not the homolysis of the Fe−O bond to form Fe^{2+} and •OOH, but the homolysis of the O−O bond to form $[Fe^{IV}O]^{2+}$ and •OH. Our ESR study results (**Figure 4c**) showing no detectable $O_2^{\bullet-}$ are in agreement with Ensing and others (*56*), supporting the homolysis of the O−O bind to form $[Fe^{IV}O]^{2+}$ and •OH under the experimental conditions.

In addition to the advantage of generating pure •OH, the ferric iron/H_2O_2 system has physiological relevance. Ferric iron is predominately found in the body bound to ferritin and tranferritin proteins. It also likely exists in the free iron pool, also referred to as the "labile iron pool," as ferric iron chelated by biological chelators such as ADP, ATP, GTP, or citrate. This "free" iron pool is thought to be available for pathological free radical reactions (*60*). In vivo studies have demonstrated that rats exposed to Fe(III) chelated with NTA caused renal carcinoma and induced DNA lesions (*1*), supporting the role of Fe(III) in oxidative reaction under physiological conditions. Given its physiological relevance and superior •OH-generating properties under physiological pH found in this study and supported by the conclusions of other researchers, the ferric iron/H_2O_2 system was chosen as the •OH-generating system for the new assay.

Detection Probe Selection. Numerous detection probes, another critical component of free radical scavenging assays, have been developed for monitoring •OH concentration and •OH scavenging capacity. These probes, including 2-deoxyribose/"TBA-reactive" substances (*17*), DNA (*15*), methionine (*58*), aromatic compounds (*15*) such as salicylic acid (*23*), DMPO adducts (*20*), fluorescamine-derivatized nitroxide (*21*), fluorescein (*26*), β-phycoerythrin (*27*), coumarin derivatives (*28*), and the chemiluminescent probe, luminal (*19*), are used for different detection methods such as molecular absorbance and fluorescence, GLC, ESR, MS, or chemiluminescence, in possible combination with separation technologies including GLC, GC, and HPLC (*15*). The ESR spin-trapping methods have excellent sensitivity and specificity, but are often not carried out under biologically relevant conditions such as pH (*62*) and require expensive equipment (*63*). Chemiluminescence methods, although sensitive, utilize a transient signal, which is not ideal for scavenging capacity assays, and do not have good specificity for •OH (*25*). MS detections require expensive instruments and are difficult to implement. This left fluorescence and molecular absorption as good potential detection methods with many potential probes.

Fluorescein was chosen as the detection probe for the new HOSC assay because of its high sensitivity to •OH attack, high quantum yield, no interferences with phenolic compounds, photostability, stability under physiological pH, wide acceptability in radical scavenging capacity assays such as the popular ORAC method (*38*), availability and reasonable cost.

Evidence of Definite Endpoint for HOSC. A definite endpoint is critical for quantification of •OH scavenging capacity. The fluorescence decay curves of fluorescein with different Trolox concentrations were determined using the ferric iron/H_2O_2 •OH-generating system in pH 7.4 phosphate buffer

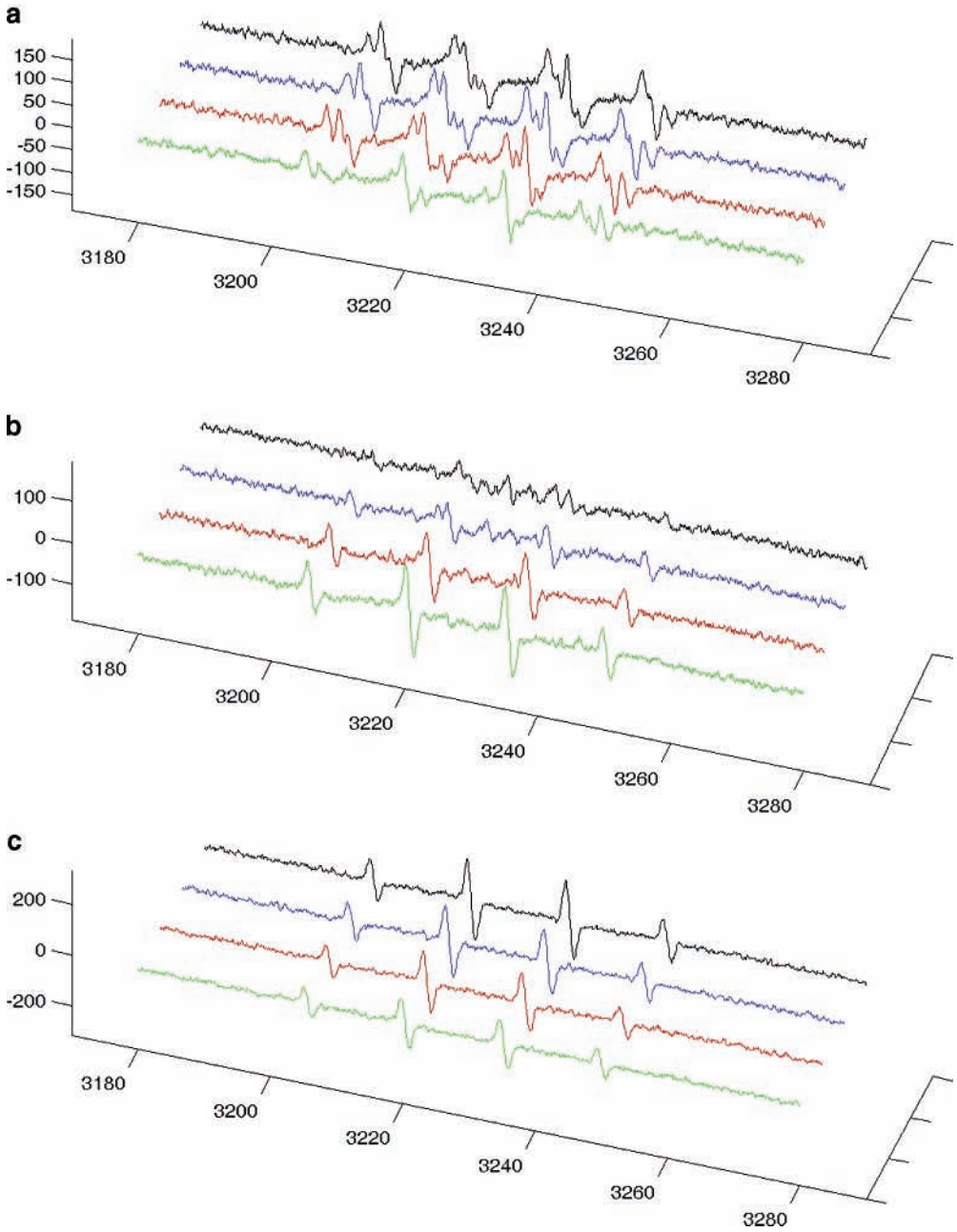

Figure 4. Reactive oxygen species generated by the (**a**) Co(II)/H_2O_2, (**b**) Cu(II)/H_2O_2, and (**c**) Fe(III)/H_2O_2 Fenton-like reaction systems. (**a**) Reactive oxygen species were determined with an ESR method using DMPO as the spin-trapping agent with the following initial reaction concentrations: 42.5 mM sodium phosphate buffer (pH 7.4), 0.1 M DMPO, 230 μM Co(II), 2.75×10^{-2}M H_2O_2, and 5% (v/v) acetone. (**b**) Reactive oxygen species were determined with an ESR method using DMPO as the spin-trapping agent with the following initial reaction concentrations: 42.5 mM sodium phosphate buffer (pH 7.4), 0.1 M DMPO, 0.95 mM Cu(II), 26.5 mM H_2O_2, and 5% (v/v) acetone. (**c**) Reactive oxygen species were determined with an ESR method using DMPO as the spin-trapping agent with the following initial reaction concentrations: 42.5 mM sodium phosphate buffer (pH 7.4), 0.1 M DMPO, 0.686 mM Fe(III), 26.5 mM H_2O_2, 5% (v/v) acetone. Measurements taken at 0, 9, 18, and 30 min are indicated by the colors green, red, blue, and black, respectively. Spectra show typical quartet signals with an intensity ratio of 1:2:2:1 ($a_N = a_H = 14.7$ G).

(**Figure 5**). Trolox is a known free radical scavenging compound that is a commonly used as an antioxidant standard in other free radical scavenging capacity assays including the popular ORAC. The decay curves clearly showed a dose-dependent lag phase inhibition of Trolox, similar to that observed for Trolox in the ORAC assay (*38*), indicating the potential of this new assay in quantifying the •OH scavenging capacity of antioxidant preparations.

Scavenging activities for the HOSC assay are calculated using the net AUC as used in other established assays such as ORAC (*38*). This method for calculating HOSC takes into account both inhibition time and extent and utilizes a definite endpoint. This is especially important as antioxidants have complex kinetics, some exhibiting a lag phase while others do not. This AUC calculation method is therefore viewed as being superior to percent inhibition or fixed time point calculations (*14*, *64*).

Confirmation of HOSC Scavenging Measurement against Pure •OH. To verify that the HOSC assay does measure scavenging activity against pure •OH, an ESR spin-trapping assay was performed with both antioxidant standards and natural extracts with results shown in **Figure 6**. These ESR results clearly show scavenging activities of these compounds and extracts, and the presence of only •OH in the reaction mixtures (**Figure 6**). Furthermore, these ESR results showed an order of

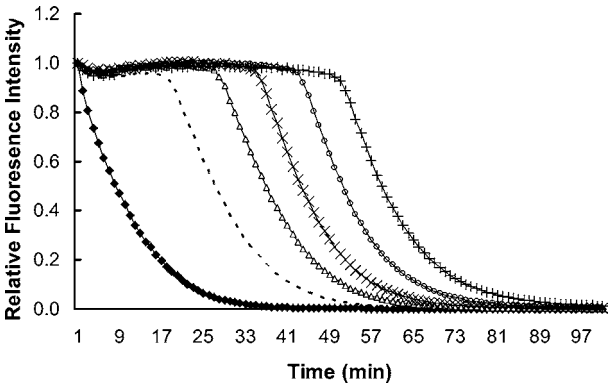

Figure 5. Fluorescence decay curve of fluorescein in the presence of Trolox under the HOSC assay condition. Initial concentrations in the reaction mixtures were 5.26×10^{-8} M FL, 42.5 mM sodium phosphate buffer, 26.53 mM H_2O_2, 0.686 mM $FeCl_3$, and 10% (v/v) Trolox solution or blank prepared in 50% acetone at the following concentrations: (■) blank containing no Trolox; (–) 20 μM; (△) 40 μM; (×) 60 μM; (○) 80 μM; (+) 100 μM Trolox.

the •OH scavenging activity similar to that obtained by the HOSC method (**Figures 6** and **7**; **Table 1**).

Correlation between HOSC and ORAC Values. The HOSC and ORAC values of the five selected phenolic acids are presented in **Figure 7**. The greater value of TE per micromole of phenolic acid is associated with a stronger HOSC or ORAC. Strong correlation ($r = 0.954$, $P = 0.05$) was observed between HOSC and ORAC values of the five antioxidative phenolic acids. Also noted was that the trend seen from these two assays in **Figure 7** agrees with results from Zhou and others (*65*), who studied the •OH scavenging activities of coumaric, ferulic, syringic, and vanillic acids using an ESR spin-trapping method and found coumaric acid to have the strongest activity.

Effect of Extraction Solvent on HOSC. One of the criteria for a potential assay was compatibility of the assay with different solvents. The effects of commonly used extraction solvents including acetone, ethanol, methanol, DMSO, and these in combination with β-cyclodextrin (RMCD) were evaluated using the HOSC assay, and results are shown in **Figure 8**. RMCD was included because of its application as solubility enhancer for antioxidant activity evaluation in aqueous phase. Results indicated that 50% acetone, a commonly used solvent for extracting phenolics (*37*), had almost no effect on the kinetics of FL degradation by •OH, whereas the remaining solvents (ethanol, methanol, and DMSO) all showed very different kinetics with almost no FL degradation, suggesting that acetone has little interference with HOSC assay and aqueous acetone is a better choice of solvent for HOSC determination. Furthermore, adding RMCD to 50% acetone significantly slowed the degradation of FL compared to 50% acetone without RMCD. The effect of RMCD on the degradation of FL for the remaining solvents showed no effect for DMSO and a slight increase for ethanol and methanol.

To further understand the solvent effect on the HOSC assay, an ESR spin-trapping assay with DMPO was conducted. ESR spectra of DMPO adducts (**Figure 9**) indicated the formation of carbon-centered radicals when ethanol, methanol, and DMSO were included in the HOSC assay, whereas •OH was the only radical in the testing system containing acetone. These carbon-centered radicals are likely formed due to proton abstraction from ethanol, methanol, and DMSO. These results were expected as ethanol, methanol, and DMSO are known to be excellent •OH scavengers and are known to form carbon-

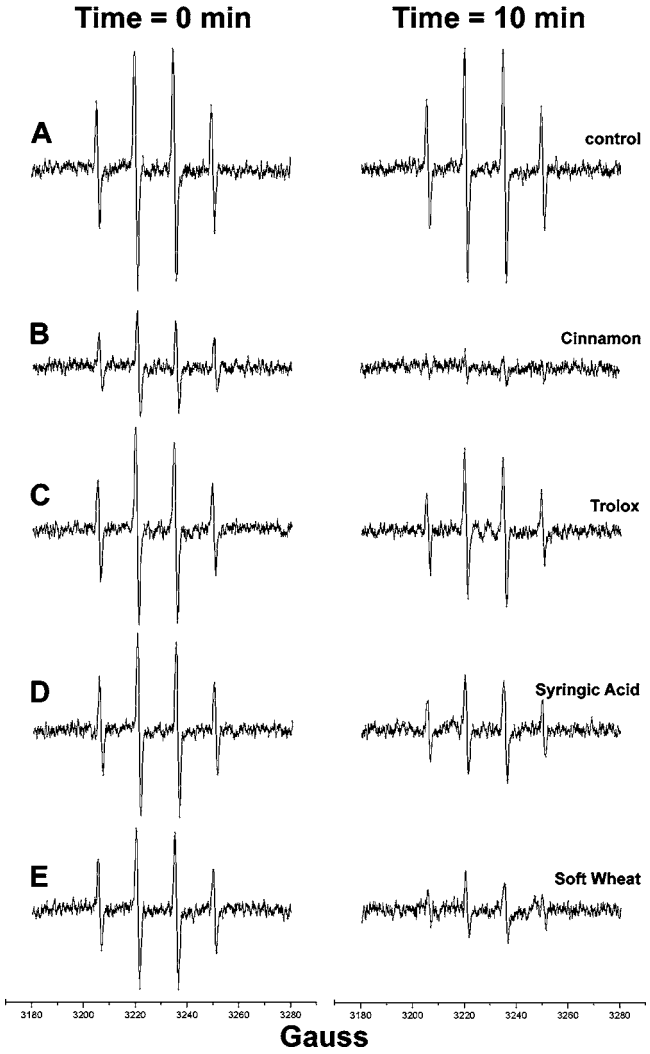

Figure 6. Scavenging activity of antioxidants and natural extracts using ESR DMPO spin-trapping assay with Fe(III)/H_2O_2. Initial reaction concentrations were 42.5 mM sodium phosphate buffer (pH 7.4), 0.1 M DMPO, 0.686 mM Fe(III), 26.5 mM H_2O_2, and 10% (v/v) standards or extracts all prepared in 50% acetone as follows: (**A**) blank, (**B**) 0.1 mg/mL cinnamon extract, (**C**) 20 mM Trolox, (**D**) 20 mM syringic acid, and (**E**) 0.1 mg/mL whole grain soft wheat extract. Measurements were taken at 0 and 10 min.

centered radicals such as α-hydroxyethyl and hydroxymethyl radicals from ethanol and DMSO or methanol, respectively, which can be spin-trapped and are often used as detecting molecules in •OH assays (*15*, *64*). These results also further support the earlier notion that the Fe(III)/H_2O_2 system is a source of •OH but not $O_2^{\bullet -}$, as the latter does not exhibit these properties (*66*).

The effect of RMCD in combination with acetone was also investigated with the ESR using DMPO as the spin-trapping agent, and results showed a significant decrease in the signal intensity of DMPO/•OH adduct with RMCD, indicating that RMCD was able to inhibit the generation of •OH under the experimental conditions or that it may react with and quench •OH with a possibility of forming radicals that were not trappable with DMPO (**Figure 9**). These results confirm the interference of RMCD on HOSC measurements, which may reduce the sensitivity of HOSC measurements. In summary, only water and acetone are compatible with the HOSC assay. It should be pointed out that these solvent compatibility issues

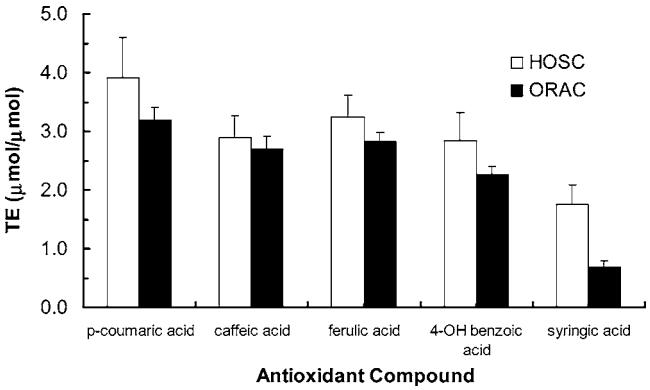

Figure 7. HOSC and ORAC values of five phenolic acids. Initial reaction concentrations for HOSC assay were 5.26×10^{-8} M FL, 42.5 mM sodium phosphate buffer, 26.53 mM H_2O_2, 0.686 mM $FeCl_3$, and individual phenolic acids at 2.5 μM. Initial reaction concentrations for the ORAC assay were 0.067 μM FL, 53.6 mM AAPH, and individual phenolic acids at 2.7 μM. Results are reported as micromoles of Trolox equivalents (TE) per micromole of phenolic acid. All tests were conducted in triplicates with mean values reported. The vertical bars represent the standard deviation of each data point ($n = 3$).

Table 1. HOSC Values for Natural Extracts

food extract	HOSC (TE)[a]	SD[b]
soft wheat	38.78	7.19
hard wheat bran	74.91	8.18
cinnamon	3009.85	233.72

[a] TE, Trolox equivalents expressed as micromoles of Trolox per gram of material. [b] SD, standard deviation.

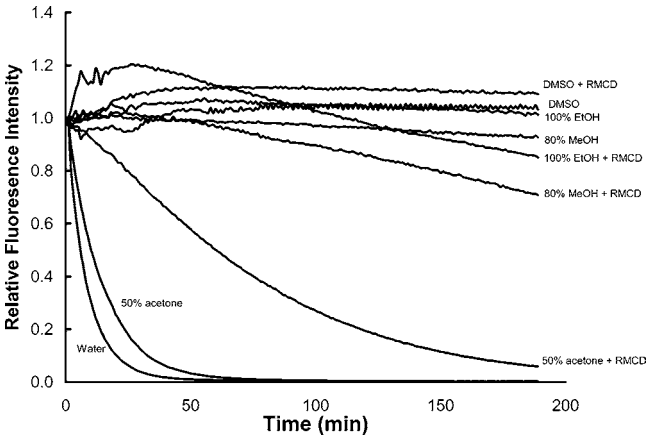

Figure 8. Effect of organic solvents and β-cyclodextrin on fluorescein degradation in HOSC assay. Initial reaction concentrations for HOSC assay were 5.26×10^{-8} M FL, 42.5 mM sodium phosphate buffer, 26.53 mM H_2O_2, 0.686 mM $FeCl_3$, and 10% (v/v) of the following solvents: water, 50% acetone, 80% methanol (MeOH), 100% ethanol (EtOH), 100% dimethyl sulfoxide (DMSO), and the above with β-cyclodextrin at 1.4% (w/v) (RMCD).

should be expected for any •OH assay and not only for the HOSC because of the chemical nature of •OH and these solvents.

Linearity and Range of HOSC Assay. A linear relationship between AUC and antioxidant concentration is important for HOSC value measurement. The linear relationship for a group of pure antioxidant compounds and botanical extracts including Trolox, ferulic acid, *p*-coumaric acid, soft wheat extract, and cinnamon extract, all known free radical scavengers, is shown in **Table 2**. Trolox was chosen as the antioxidant standard to express other antioxidants for this assay because of its excellent linear relationship ($R^2 = 0.99$) and sensitivity (slope = 0.4) under the experimental conditions and its wide use as a standard in other assays such as ORAC. HOSC values were therefore expressed as TE per unit of testing sample. The linear range for Trolox was found between 20 and 100 μM in the testing solution.

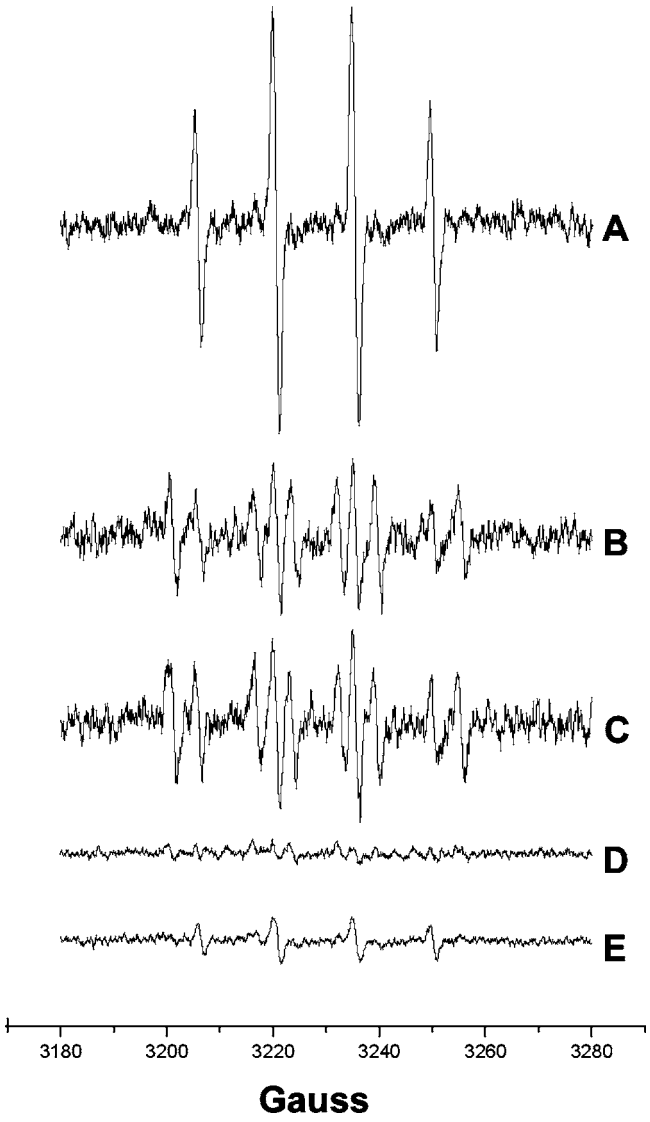

Figure 9. ESR spectra of DMPO–ROS adducts observed in the presence of different solvents and β-cyclodextrin using Fe(III)/H_2O_2 as •OH-generating system. Initial reaction concentrations were 42.5 mM phosphate buffer (pH 7.4), 0.1 M DMPO, 0.686 mM Fe(III), 26.5 mM H_2O_2, and 10% (v/v) of the following solvents: (**A**) 50% acetone, (**B**) 100% ethanol (EtOH), (**C**) 80% methanol (MeOH), (**D**) 100% dimethyl sulfoxide (DMSO), and (**E**) 50% acetone and 1.4% (w/v) β-cyclodextrin (RMCD).

Table 2. Linear Relationships between Antioxidant Concentration and Net Area under the Curve Using HOSC Assay[a]

compound	concn range	R^2	slope	*y*-intercept
Trolox	20–100 μM	0.993	0.400	9.595
p-coumaric acid	2–40 μM	0.995	1.671	0.928
ferulic acid	2–60 μM	0.994	1.369	6.201
soft wheat	0.770–2 μg/mL	0.968	22.182	0.177
cinnamon	83.3–200 ng/mL	0.979	462.430	30.808

[a] All measurements were conducted under HOSC assay conditions with antioxidant and botanical extracts in 50% acetone. All tests were conducted in triplicate.

Table 3. Precision and Accuracy of Quality Control (QC) Samples

	QC1	QC2	QC3
nominal [Trolox] (μM)	60	80	100
run 1			
intramean (μM)	61.58	81.82	96.63
SD[a]	2.36	11.02	10.45
%RSD[b]	3.84	13.47	10.82
%REC[c]	102.63	102.27	96.63
n	3	3	3
run 2			
intramean (μM)	60.83	85.50	94.91
SD	5.26	6.79	10.31
%RSD	8.65	7.94	10.87
%REC	101.39	106.87	94.91
n	3	3	3
run 3			
intramean (μM)	62.82	81.58	96.91
SD	1.63	8.48	8.71
%RSD	2.60	10.40	8.98
%REC	104.70	101.97	96.91
n	3	3	3
pooled runs			
intermean (μM)	61.74	82.97	96.15
SD	3.12	7.97	8.59
%RSD	5.06	9.60	8.93
%REC	102.90	103.71	96.15
n	9	9	9

[a] SD, standard deviation. [b] %RSD, percent relative standard deviation. [c] %REC, percent recovery.

Reproducibility, Accuracy, and Precision of HOSC Assay. The day-to-day reproducibility of the HOSC method was assessed using a 25 μM caffeic acid standard measured six times in triplicate over 12 days. Results showed an average TE value of 4.16 and percent relative standard deviation (%RSD) of 4.06% during the testing time frame (data not shown), suggesting that the HOSC procedure is stable for day-to-day measurements. The accuracy and precision of the method were evaluated by comparing three runs of Trolox at three concentrations within a day. **Table 3** summarizes the results and indicates a pooled precision measured as %RSD within $\pm$15% and pooled accuracy measured as percent recovery (%REC) between 96 and 104%.

Conclusion. A novel hydroxyl radical scavenging capacity assay named HOSC was described and validated. The HOSC assay measures the scavenging capacity of antioxidant samples against a constant flux of pure hydroxyl radicals under physiological pH, with a definite endpoint. This method uses an inexpensive stable common fluorescent probe and may be performed with a plate reader with a fluorescence detector for high-throughput analyses or scaled up and adapted to a single-read fluorometer. The HOSC assay is compatible with water and acetone extracts and has excellent correlation with a popular radical scavenging capacity assay (ORAC). Finally, the HOSC assay has acceptable sensitivity, ruggedness, precision, and accuracy. Compared to the commonly used deoxyribose method, the HOSC method has better compatibility with acetone and more efficiently generates hydroxyl radicals under physiological pH. The HOSC method may serve as an important tool for those researchers interested in the radical scavenging capacities of both food extracts and pure antioxidant compounds with applications in the food, biological, and medical fields.

LITERATURE CITED

(1) Kawanishi, S.; Hiraku, Y.; Murata, M.; Oikawa, S. The role of metals in site-specific DNA damage with reference to carcinogensis. *Free Radical Biol. Med.* **2002**, *32*, 822−832.

(2) Sachidanandame, K.; Fagan, S. C.; Ergul, A. Oxidative stress and cardiovascular disease: antioxidants and unresolved issues. *Cardiovasc. Drug Rev.* **2005**, *23*, 115−32.

(3) Bodamyali, T.; Stevens, C. R.; Blake, D. R.; Winyard, P. G. Reactive oxygen/nitrogen species and acute inflammation: a physiological process. In *Free Radicals and Inflammation*, 1st ed.; Winyard, P. G., Blake, D. R., Evans, C. H., Eds.; Birkhauser: Basel, Switzerland, 2000; pp 11−19.

(4) Butterfield, D. A. Alzheimer's β-amyloid peptide and free radical oxidative stress. In *Reactive Oxygen Species in Biological Systems: An Interdisciplinary Approach*, 1st ed.; Gilbert, D. L., Colton, C. A., Eds.; Kluwer Academic Publishers: New York, 1999; pp 609−638.

(5) Cohen, G. Oxidative stress and Parkinson's disease. In *Reactive Oxygen Species in Biological Systems: An Interdisciplinary Approach*, 1st ed.; Gilbert, D. L., Colton, C. A., Eds.; Kluwer Academic Publishers: New York, 1999; pp 593−608.

(6) Niedowicz, D. M.; Daleke, D. L. The role of oxidative stress in diabetic complications. *Cell Biochem. Biophys.* **2005**, *43*, 289−330.

(7) Rajindar, S. S.; Mockett, R. J.; Orr, W. C. Mechanisms of aging: an appraisal of the oxidative stress hypothesis. *Free Radical Biol. Med.* **2002**, *33*, 575−586.

(8) Stadtman, E. R.; Berlett, B. S. Reactive-oxygen mediated protein oxidation in aging and disease. *Chem. Res. Toxicol.* **1997**, *10*, 485−494.

(9) Poli, G.; Leonarduzzi, U.; Biasi, F.; Chiarpotto, E. Oxidative stress and cell signaling. *Curr. Med. Chem.* **2004**, *11*, 1163−1182.

(10) Evans, M. D.; Dizdaroglu, M.; Cooke, M. S. Oxidative DNA damage and disease: induction, repair and significance. *Mutat. Res.* **2004**, *567*, 1−61.

(11) Crawford, D. R. Regulation of mammalian gene expression by reactive oxygen species. In *Reactive Oxygen Species in Biological Systems: An Interdisciplinary Approach*, 1st ed.; Gilbert, D. L., Colton, C. A., Eds.; Kluwer Academic Publishers: New York, 1999; pp 155−171.

(12) Shi, H.; Hudson, L. G.; Liu, K. J. Oxidative stress and apoptosis in metal ion-induced carcinogenesis. *Free Radical Biol. Med.* **2004**, *37*, 582−593.

(13) Willcox, J. K.; Ash, S. L.; Catignani, G. L. Antioxidants and prevention of chronic disease. *Crit. Rev. Food Sci.* **2004**, *44*, 275−295.

(14) Prior, R. L.; Wu, X. L.; Schaich, K. Standardized methods for the determination of antioxidant capacity and phenolics in foods and dietary supplements. *J. Agric. Food Chem.* **2005**, *53*, 4290−4302.

(15) Halliwell, B., Gutteridge, J. M. C., Eds. The chemistry of oxygen radicals and other oxygen-derived species. In *Free Radicals in Biology and Medicine*, 3rd ed.; Oxford University Press: New York, 1989; pp 22−81.

(16) Lubec, G. The hydroxyl radical: from chemistry to human disease. *J. Invest. Med.* **1996**, *44*, 324−346.

(17) Aruoma, O. I. Deoxyribose assay for detecting hydroxyl radicals. In *Oxygen Radicals in Biological Systems, Part C. Methods in Enzymology*, 1st ed.; Packer, L., Ed.; Academic Press: San Diego, CA, 1994; Vol. 233, pp 57−66.

(18) Wang, S. Y.; Zheng, W. Effect of plant growth temperature on antioxidant capacity in strawberry. *J. Agric. Food Chem.* **2001**, *49*, 4977−4982.

(19) Hirayama, O.; Yida, M. Evaluation of hydroxyl radical-scavenging ability by chemiluminescence. *Anal. Biochem.* **1997**, *251*, 297−299.

(20) Madsen, H. L.; Nielsen, B. R.; Bertelsen, G.; Skibsted, L. H. Screening of antioxidative activity of spices. A comparison between assays based on ESR spin trapping and electrochemical measurement of oxygen consumption. *Food Chem.* **1996**, *57*, 331−337.

(21) Li, B.; Gutierrez, P. L.; Blough, N. V. Trace determination of hydroxyl radical in biological systems. *Anal. Chem.* **1997**, *69*, 4295−4302.

(22) Chen, R.; Stenken, J. A. An in vitro hydroxyl radical generation assay for microdialysis sampling calibration. *Anal. Biochem.* **2002**, *306*, 40−49.
(23) Owen, R. W.; Wimonwatwatee, T.; Spiegelhalder, B.; Bartsch, H. A high performance liquid chromatography system for quantification of hydroxyl radical formation by determination of dihydroxy benzoic acids. *Eur. J. Cancer Prev.* **1996**, *5*, 233−240.
(24) Richmond, R.; Halliwell, B.; Chauhan, J.; Darbre, A. Superoxide-dependent formation of hydroxyl radicals: detection of hydroxyl radicals by the hydroxylation of aromatic compounds. *Anal. Biochem.* **1981**, *139*, 487−492.
(25) Yang, X.; Guo, X. Fe(II)-EDTA chelate-induced aromatic hydroxylation of terephthalate as a new method for the evalution of hydroxyl radical-scavenging ability. *Analyst* **2001**, *126*, 928−932.
(26) Ou, B.; Hampsch-Woodill, M.; Flanagan, J.; Deemer, E. K.; Prior, R. L.; Huang, D. J. Novel fluorometric assay for hydroxyl radical prevention capacity using fluorescein as the probe. *J. Agric. Food Chem.* **2002**, *50*, 2772−2777.
(27) Cao, G.; Sofic, E.; Prior, R. L. Antioxidant and prooxidant behavior of flavonoids: structure−activity relationships. *Free Radical Biol. Med.* **1997**, *22*, 749−760.
(28) Markigiorgos, G. M.; Bump, E.; Huang, C.; Baranowska-Kortylewicz, J.; Kassis, A. I. A fluorometric method for the detection of copper-mediated hydroxyl free radicals in the immediate proximity of DNA. *Free Radical Biol. Med.* **1995**, *18*, 669−678.
(29) Tobin, D.; Arvanitidis, M.; Bisby, R. H. One-electron oxidation of "photo-Fenton" reagents and inhibition of lipid peroxidation. *Biochem. Biophys. Res. Commun.* **2002**, *299*, 155−159.
(30) Dorman, H. J. D.; Bachmayer, O.; Kosar, M.; Hiltunen, R. Antioxidant properties of aqueous extracts from selected Lamiaceae species grown in Turkey. *J. Agric. Food Chem.* **2004**, *52*, 762−770.
(31) Daglia, M.; Racchi, M.; Papetti, A.; Lanni, C.; Govoni, S.; Gazzani, G. In vitro and ex vivo antihydroxyl radical activity of green and roasted coffee. *J. Agric. Food Chem.* **2004**, *52*, 1700−1704.
(32) Zou, Y. P.; Lu, Y. H.; Wei, D. Z. Antioxidant activity of a flavonoid-rich extract of *Hypericum perforatum* L. in vitro. *J. Agric. Food Chem.* **2004**, *52*, 5032−5039.
(33) Martinez-Tome, M.; Murcia, M. A.; Frega, N.; Ruggieri, S.; Jimenez, A. M.; Roses, F.; Parras, P. Evaluation of antioxidant capacity of cereal brans. *J. Agric. Food Chem.* **2004**, *52*, 4690−4699.
(34) Tadolini, B.; Cabrini, L. The influence of pH on OH. Scavenger inhibition of damage to deoxyribose by Fenton reaction. *Mol. Cell. Biochem.* **1990**, *94*, 97−104.
(35) Welch, K. D.; Davis, T. Z.; Aust, S. D. Iron autoxidation and free radical generation: effects of buffers, ligands, and chelators. *Arch. Biochem. Biophys.* **2002**, *397*, 360−369.
(36) Cohen, G. The Fenton reaction. In *Handbook of Methods of Oxygen Radical Research*, 1st ed.; Greenwald, R. A., Ed.; CRC Press: Boca Raton, FL, 1985; pp 55−64.
(37) Moore, J.; Hao, Z.; Zhou, K.; Luther, M.; Costa, J.; Yu, L. Carotenoid, tocopherol, phenolic acid, and antioxidant properties of Maryland-grown soft wheat. *J. Agric. Food Chem.* **2005**, *53*, 6649−6657.
(38) Ou, B. X.; Hampsch-Woodill, M.; Prior, R. L. Development and validation of an improved oxygen radical absorbance capacity assay using fluorescein as the fluorescent probe. *J. Agric. Food Chem.* **2001**, *49*, 4619−4625.
(39) Tachon, P. Ferric and cupric ions requirement for DNA single-strand breakage by H_2O_2. *Free Radical Res. Commun.* **1989**, *7*, 1−10.
(40) Kocha, T.; Yamaguchi, M.; Ohtaki, H.; Fukuda, T.; Aoyagi, T. Hydrogen peroxide-mediated degradation of protein: different oxidation modes of copper- and iron-dependent hydroxyl radicals on the degradation of albumin. *Biochim. Biophys. Acta* **1997**, *1337*, 319−326.
(41) Goldstein, S.; Meyerstein, D. Comments on the mechanism of the "Fenton-like" reaction. *Acc. Chem. Res.* **1999**, *32*, 547−550.
(42) Liochev, S. I. The mechanism of "Fenton-like" reactions and their importance for biological systems. A biologist's view. In *Interrelations between Free Radicals and Metal Ions in Life Processes. Metal Ions in Biological Systems*, 1st ed.; Sigel, A., Sigel, H., Eds.; Dekker: New York, 1999; Vol. 36, pp 1−31.
(43) Zhao, H.; Joseph, J.; Zhang, H.; Karou, H.; Kalyanaraman, B. Synthesis and biochemical applications of a solid cyclic nitrone spin trap: a relatively superior trap for detecting superoxide anions and glutathiyl radicals. *Free Radical Biol. Med.* **2001**, *31*, 599−601.
(44) Kadiiska, M. B.; Maples, K. R.; Mason, R. P. A comparison of cobalt(II) and iron(II) hydroxyl and superoxide free radical formation. *Arch. Biochem. Biophys.* **1989**, *275*, 98−111.
(45) Leonard, S.; Gannett, P. M.; Rojanasakul, Y.; Schwegler-Berry, D.; Castranova, V.; Vallyathan, V.; Shi, X. Cobalt-mediated generation of reactive oxygen species and its possible mechanisms. *J. Inorg. Biochem.* **1998**, *70*, 239−244.
(46) Yamamoto, K.; Inoue, S.; Yamazaki, A.; Yoshinaga, T.; Kawanishi, S. Site-specific DNA damage induce by cobalt(II) ion and hydrogen peroxide: role of singlet oxygen. *Chem. Res. Toxicol.* **1989**, *2*, 234−239.
(47) Hanna, P.; Kadiiska, M.; Mason, R. P. Oxygen-derived free radical and active oxygen complex formation from cobalt(II) chelates in vitro. *Chem. Res. Toxicol.* **1992**, *5*, 109−115.
(48) Li, Y.; Trush, M. A. Reactive oxygen DNA damage resulting from the oxidation of phenolic compounds by a copper-redox cycle mechanism. *Cancer Res.* **1994**, *54S*, 1895s−1898s.
(49) Frelon, S.; Douki, T.; Favier, A.; Cadet, J. Hydroxyl radical not the main reactive species involved in the degradation of DNA bases by copper in the presence of hydrogen peroxide. *Chem. Res.* **2003**, *16*, 191−197.
(50) Yamamoto, K.; Kawanish, S. Hydroxyl free radical is not the main active species in site-specific DNA damage induced by copper(II) ion and hydrogen peroxide. *J. Biol. Chem.* **1989**, *264*, 15435−15440.
(51) Zhu, B. Z.; Zhao, H. T.; Kalyanaraman, B.; Frei, B. Metal-independent production of hydroxyl radicals by halogenated quinines and hydrogen peroxide: an ESR spin trapping study. *Free Radical Biol. Med.* **2002**, *32*, 465−473.
(52) Zhang, D.; Yasuda, T.; Yu, Y.; Zheng, P.; Kawabata, T.; Ma, Y.; Okada, S. Ginseng extract scavenges hydroxyl radical and protects unsaturated fatty acids from decomposition caused by iron-mediated lipid peroxidation. *Free Radical Biol. Med.* **1996**, *20*, 145−150.
(53) Gutteridge, J. M. C.; Maidt, L.; Poyer, L. Superoxide dismutase and Fenton chemistry. *Biochem. J.* **1990**, *269*, 169−174.
(54) Awai, M. Pathogenesis and mechanism of iron overload: ferric nitrilotriacetate, hemosiderin, active oxygen, and carcinogenesis. *Rinsho Ketsueki* **1989**, *30*, 1115−1127.
(55) De Laat, J.; Le, T. G. Kinetics and modeling of the Fe(III)/H_2O_2 system in the presence of sulfate in acidic aqueous solutions. *Environ. Sci. Technol.* **2005**, *39*, 1811−1818.
(56) Ensing, B.; Buda, F.; Baerends. Fenton-like chemistry in water: oxidation catalysis by Fe(III) and H_2O_2. *J. Phys. Chem. A* **2003**, *107*, 5722−5731.
(57) Barb, W. G.; Baxendale, J. H.; George, P.; Hargrave, K. R. Reactions of ferrous and ferric ions with hydrogen peroxide. Part II—the ferric ion reaction. *Trans. Faraday Soc.* **1951**, *47*, 951−616.
(58) Perez-Benito, J. F. Iron(III)-hydrogen peroxide reaction: kinetic evidence of a hydroxyl-mediated chain mechanism. *J. Phys. Chem. A* **2004**, *108*, 4853−4858.
(59) De Laat, J.; Gallard, H. Catalytic decomposition of hydrogen peroxide by Fe(III) in homogeneous aqueous solution: mechanism and kinetic modeling. *Environ. Sci. Technol.* **1999**, *33*, 2726−2732.
(60) Toyokuni, S. Iron-induced carcinogenesis: the role of redox regulation. *Free Radical Biol. Med.* **1996**, *20*, 553−566.

(61) Lawrence, G. D. Ethylene formation from methionine and its analogs. In *Handbook of Methods of Oxygen Radical Research*, 1st ed.; Greenwald, R. A., Ed.; CRC Press: Boca Raton, FL, 1985; pp 157−163.
(62) Stephanson, C. J.; Stephanson, A. M.; Flanagan, G. P. Evaluation of hydroxyl radical-scavening abilities of silica hydride, and antioxidant compound, by Fe^{2+}-EDTA-induced 2-hydroxytereph-thalate fluorometric analysis. *J. Med. Food* **2003**, *6*, 249−253.
(63) Castro, J. A.; Castro, G. D. Hydroxyl and 1-hydroxyethyl radical detection by spin trapping and GC-MS. In *Oxidative Stress Biomarkers and Antioxidant Protocols*, 1st ed.; Armstrong, D., Ed.; Humana Press: Totowa, NJ, 2002; pp 89−98.
(64) Huang, D.; Ou, B.; Prior, R. L. The chemistry behind antioxidant capacity assays. *J. Agric. Food Chem.* **2005**, *53*, 1841−1856.
(65) Zhou, K.; Yin, J.; Yu, L. ESR determination of the reactions between selected phenolic acids and free radicals or transition metals. *Food Chem.* **2005**, in press.
(66) Rosen, G. M.; Pou, S.; Britigan, B. E.; Cohen, S. C. Spin trapping of hydroxyl radicals in biological systems. In *Oxygen Radicals in Biological Systems, Part C. Methods in Enzymology*, 1st ed.; Packer, L., Ed.; Academic Press: San Diego, CA, 1994; Vol. 233, pp 105−111.

Received for review October 14, 2005. Revised manuscript received December 8, 2005. Accepted December 13, 2005. This research was supported by the USDA-CSREES National Research Initiatives under Federal Grant 20043550314852, the Maryland Grain Producers Utilization Board (MGPUB) under MGPUB Grant 205198, and the Maryland Agricultural Experiment Station.

JF052555P